Manganese-II Oxidation: A Biotic and Abiotic Process

The oxidation of Mn(II) to form nanocrystalline Mn(III/IV) oxides has sweeping environmental ramifications, impacting the fate and transport of contaminants and degradation of carbon. The homogenous oxidation of Mn(II) by O_2 is a thermodynamically favorable process, but is kinetically limited in the absence of catalysts. The rates of Mn(II) oxidation are much higher for surface catalyzed, heterogeneous reactions, with half lives of Mn(II) ranging from 5 to 2800 d for surface catalyzed oxidation. Bacterially mediated oxidation has been reported as ~5 orders of magnitude higher than surface catalyzed abiotic reactions and, thus, bacterial Mn(II) oxidation is considered to be a primary means of Mn oxide formation in the environment. While the majority of microbial Mn(II) oxidation has been attributed to direct enzymatic activity, the biochemical and genetic mechanisms involved in this oxidation are still poorly understood.

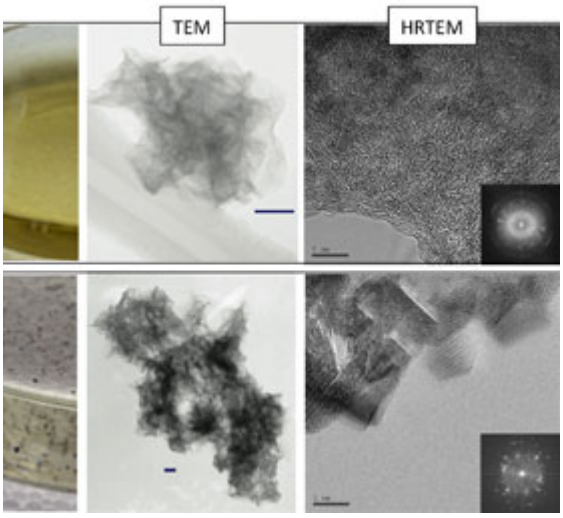

Figure 1. Mn oxides formed in the cell-free filtrate after 24 (top) and 96 hours (bottom) of oxidation. Left panel is a picture of the reacted filtrate within 125 ml flasks – the 24 hour filtrate has a brown turbidity that disappears once discrete Mn oxide particles are observed. The middle and right panels are TEM images of the minerals, illustrating the presence of dispersed, individual Mn oxides particles after 24 hours and more crystalline Mn oxide particle aggregates after 96 hours of oxidation. Scale bar = 20 nm.

Recently, we have expanded the role of bacteria in Mn(II) oxidation to include a novel indirect oxidation pathway involving extracellular superoxide. Specifically, *Roseobacter* sp. AzwK-3b rapidly oxidizes Mn(II) to Mn(III) within both cell cultures and cell free filtrates via the enzymatic production of superoxide [1]. Mn(III) then is either further oxidized by an unknown oxidant or disproportionates to Mn(IV). Overall rates of Mn oxide formation by *Roseobacter* AzwK-3b are enhanced in the presence of light [2], yet the production rate of the intermediate Mn(III) does not vary in the light versus dark [1]. Considering the chemical and photochemical reactivity of Mn oxides (particularly those that are nanoparticulate), these results suggest that the Mn oxide products themselves are contributing to Mn(II) oxidation by *Roseobacter* sp. AzwK-3b. When proteases (enzymes that inactivate proteins) were added to cell free filtrate incubations containing aqueous Mn(II) within the first 12 hours of reaction, Mn(II) oxidation was completely inhibited. However, if proteases were added after 12 hours, Mn(II) oxidation continued uninhibited until ~30 hours. These results together pointed to a combination of superimposed biological (enzymatic superoxide) and mineral-induced Mn(II) oxidation pathways.

In a recent study published in *Geochimica et Cosmochimica Acta* [3], we used a combination of microscopic (high resolution transmission electron microscopy, HRTEM), spectroscopic (X-ray absorption spectroscopy, XAS) and classical kinetic experiments to elucidate the contribution of the biogenic produced Mn oxides in the overall scheme of Mn(II) oxidation. Mn oxides were formed in *Roseobacter* AzwK-3b cell free filtrates and harvested at varying time points for microscopic and spectroscopic characterization at BL 11-2. Using a Mn EXAFS structural model [4], the Mn oxide composition and structure were defined at

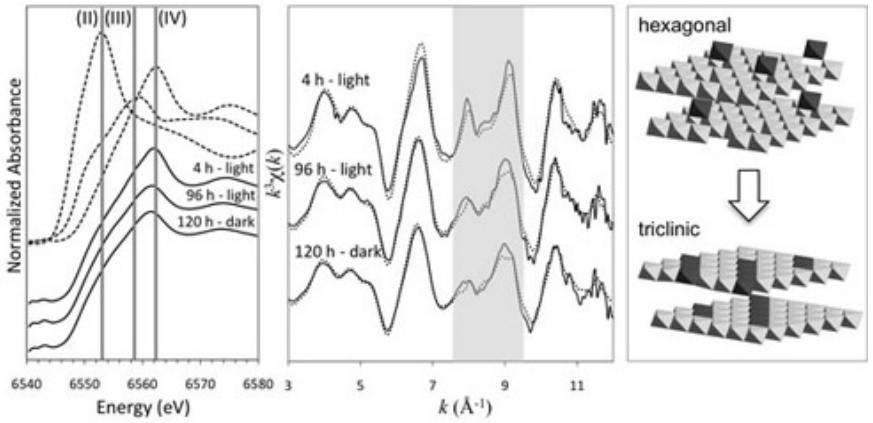

Figure 2. Mn K-edge XANES (left) and EXAFS (middle) spectra of the Mn oxides produced from the filtrate after 4 or 96 hours of oxidation in the light and 120 hours of oxidation in the dark. In the XANES figure, the dotted lines represent the standards for Mn(IV) (δ-MnO_2), Mn(III) (β-MnOOH), and Mn(II) ($MnCl_2$). The dotted lines in the EXAFS spectra are the linear-combination fit for the initial colloidal oxides (fit = 100% δ-MnO_2) formed in the light, particulate oxides formed in the light (fit = 45% δ-MnO_2, 55% triclinic birnessite) and particulate oxides formed in the dark (fit = 22% δ-MnO_2, 78% triclinic birnessite). The gray shaded area highlights the "indicator region" emphasizing the spectral differences between hexagonal and triclinic birnessite. The right panel shows simplified polyhedral representations of the birnessite crystal structures formed. The dark shaded octahedra in the birnessite structures represent lattice positions of Mn^{3+} octahedra. Interlayer cations are omitted for simplicity.

each time point. The oxides were then reacted with aqueous Mn(II) at varying concentrations and aqueous conditions. We show that the oxidation of Mn(II) by microbially-produced extracellular O_2^- results in the formation of highly reactive colloidal (average ~40 nm diameter) hexagonal birnessite, most similar to nanocrystalline d-MnO_2 [3] (Figure 1 and 2). These colloidal oxides induce the rapid oxidation of Mn(II) with rates (average ~2.5 $\delta - M\ h^{-1}$) (Figure 3) equivalent to other mineral-catalyzed Mn(II) oxidation rates (e.g., nano-hematite rates ~4 $\mu M\ h^{-1}$ [5]) and faster than reported biological (i.e., enzymatic) rates in natural waters (e.g., ~3-12 $nM\ h^{-1}$ [6-8]). However, the reactivity of the colloidal hexagonal birnessite phase is short-lived due to rapid evolution to a more crystalline (Figure 1), triclinic birnessite phase (Figure 2), likely due to accumulation of Mn(III) (>10 mole % increase based on XANES analysis) within the layer. The secondary triclinic phase does not induce Mn(II) oxidation regardless of the aqueous conditions and instead photoreduction is observed within 24 hours (Figure 3).

These results show that the oxidation of Mn(II) involves a combination of biotic and abiotic processes, involving enzymatically produced superoxide and mineral catalysis. These coupled enzymatic and abiotic pathways are linked such that enzymatic oxidation is requisite for the mineral-induced pathway to occur. Thus, adding a protease before Mn oxide nucleation initiates will lead to erroneous conclusions as to the relative role of biotic and abiotic processes. Further, the evolution of initial reactive hexagonal birnessite to non-reactive triclinic birnessite imposes the need for continuous production of new colloidal hexagonal birnessite particles for Mn(II) oxidation to be sustained, illustrating an intimate dependency of enzymatic and mineral-based reactions in Mn(II) oxidation.

Primary Citations

Learman, D.R., S.D. Wankel, S.M. Webb, N. Martinez, A.S. Madden, C.M. Hansel. 2011. Coupled biotic-abiotic Mn(II) oxidation pathway mediates the formation and structural evolution of biogenic Mn oxides. *Geochim. Cosmochim. Acta* 75, 6048-6063.

Learman, D.R., B.M. Voelker, A.I. Vazquez-Rodriguez, and C.M. Hansel. 2011. Formation of manganese oxides by bacterially generated superoxide. *Nature Geosciences* 4, 95-98.

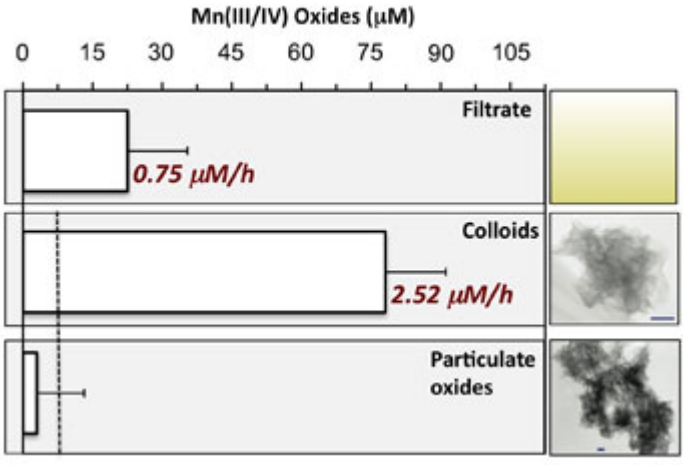

Figure 3. Comparison of Mn(II) oxide formation in the unamended filtrate (top) or filtrate amended with the initial colloidal (middle) or particulate Mn oxides (bottom). Mn oxidation experiments were run for 24 hours at 25°C in the light. Mn oxides were reacted in cell free filtrate. The rates of Mn(II) oxidation are shown adjacent to the bars (in red). The error bars represent standard deviation of three data points.

References

1. Learman, D. R.; Voelker, B. M.; Vazquez-Rodriguez, A. I.; Hansel, C. M., Formation of manganese oxides by bacterially generated superoxide. *Nature Geoscience* **2011,** *4*, 95–98.
2. Hansel, C. M.; Francis, C. A., Coupled photochemical and enzymatic Mn(II) oxidation pathways of a planktonic *Roseobacter*-Like bacterium. *Appl Environ Microbiol* **2006,** *72*, (5), 3543-9.
3. Learman, D. R.; Wankel, S. D.; Webb, S. M.; Martinez, N.; Madden, A. S.; Hansel, C. M., Coupled biotic-abiotic Mn(II) oxidation pathway mediates the formation and structural evolution of biogenic Mn oxides. *Geochim. Cosmochim. Acta* **2011**, *75,* 6048-6063.
4. Webb, S. M.; Tebo, B. M.; Bargar, J. R., Structural characterization of biogenic Mn oxides produced in seawater by the marine *Bacillus* sp. strain SG-1. *American Mineralogist* **2005,** *90*, 1342-1357.
5. Madden, A. S.; Hochella, M. F., A test of geochemical reactivity as a function of mineral size: Manganese oxidation promoted by hematite nanoparticles. *Geochimica Et Cosmochimica Acta* **2005,** *69*, (2), 389-398.
6. Dick, G. J.; Clement, B. G.; Webb, S. M.; Fodrie, F. J.; Bargar, J. R.; Tebo, B. M., Enzymatic microbial Mn(II) oxidation and Mn biooxide production in the Guaymas Basin deep-sea hydrothermal plume. *Geochimica Et Cosmochimica Acta* **2009,** *73*, (21), 6517-6530.
7. Tebo, B. M.; Emerson, S., Effect of Oxygen-Tension, Mn(II) Concentration, and Temperature on the Microbially Catalyzed Mn(II) Oxidation Rate in a Marine Fiord. *Applied and Environmental Microbiology* **1985,** *50*, (5), 1268-1273.
8. Tebo, B. M.; Emerson, S., Microbial Manganese(II) Oxidation in the Marine-Environment - a Quantitative Study. *Biogeochemistry* **1986,** *2*, (2), 149-161.

SSRL is primarily supported by the DOE Offices of Basic Energy Sciences and Biological and Environmental Research, with additional support from the National Institutes of Health, National Center for Research Resources, Biomedical Technology Program, and the National Institute of General Medical Sciences.